Front. Archit. Civ. Eng. China 2010, 4(1): 65–77
DOI 10.1007/s11709-010-0002-9

RESEARCH ARTICLE

Xiangyu XU, Dawen YANG

Analysis of catchment evapotranspiration at different scales using bottom-up and top-down approaches

© Higher Education Press and Springer-Verlag 2009

Abstract Physically-based hydrological models are used to predict catchment water balance through detailed simulation of hydrological processes at small temporal and spatial scales. However, annual catchment water balance can also be easily and simply predicted using lumped conceptual model. Comparison between physically-based hydrological models and lumped conceptual models can help us understand the dominant factors on catchment water balance at different scales. In this paper, a distributed physically-based hydrological model (i.e., bottom-up approach) and a simple water-energy balance model (i.e., top-down approach) are used to predict actual evapotranspiration in nine sub-catchments, and the whole basin of the Luan River in northern China. Both simulations give very close values of annual evapotranspiration and show the same complementary relationship between actual and potential evapotranspiration at annual time scale. From the analysis at different time scales through comparison of the top-down and the bottom-up methods, it is shown that the annual catchment evapotranspiration is controlled mainly by annual precipitation and potential evapotranspiration, and the variability of soil water and vegetation becomes more important at a smaller time scale in the study areas. It is also known that the relationship between potential and actual evapotranspiration shows a highly nonlinear relationship at the annual and catchment scale but can be simplified to a linear relationship at hourly temporal and hillslope scales, which is commonly used in the physically-based hydrological models.

Keywords catchment evapotranspiration, distributed hydrological model, water-energy balance model, top-down and bottom-up approaches

Received July 17, 2009; accepted October 13, 2009

Xiangyu XU, Dawen YANG (✉)
State Key Laboratory of Hydroscience and Engineering, Department of Hydraulic Engineering, Tsinghua University, Beijing 100084, China
E-mail: yangdw@tsinghua.edu.cn

1 Introduction

Evapotranspiration is a highly nonlinear process in catchment hydrological cycle, and the simulation of evapotranspiration process is a major component of physically-based hydrological models. Most process-based hydrological models estimate actual evapotranspiration following the Penman's approach [1,2] by reducing potential evapotranspiration to actual evapotranspiration in response to water stress, which is given by a function of soil water availability for a given vegetation condition. The soil water availability is governed by other hydrological processes, such as infiltration and soil moisture redistribution (both vertically and laterally). Physically-based hydrological model can predict catchment water balance through detailed simulation of hydrological processes at small temporal and spatial scales. However, annual catchment evapotranspiration can be easily and simply be predicted using lumped conceptual models, such as the water-energy balance model based on the Budyko hypothesis [3]. Combination of these bottom-up and top-down approaches can help understand the dominant control on catchment evapotranspiration at different time scales.

The top-down approach in hydrology was first introduced by Klemes [4] and extended further by Sivapalan et al., as outlined in Ref. [5]. This approach was used to investigate the hydrological response at long temporal scale and large spatial scale (e.g., an annual time and watershed scale) and progressively narrows down to the processes at smaller scales (e.g., hourly time and hillslope scale). The major advantage of the top-down approach is that it can reduce data requirements and limit model complexity [6]. The lumped conceptual model is a typical example. A simple lumped model can be easily used for hypothesis testing and as the starting point for developing a new generation of models. Many researchers carried out a series of studies using the top-down approach [4,7–13] and developed a collection of lumped conceptual models for simulating water balance responses across different

temporal scales (annual, monthly, and daily) in different watersheds located in different climatic regimes. Budyko [14] proposed a semi-empirical relationship between the ratio of annual evapotranspiration to annual precipitation and the ratio of annual precipitation to annual net radiation. Considerable studies have been performed on the Budyko curve [15–20] through analyzing the interactions between climate, soils, and vegetation in producing annual water balance. A simple water-energy balance equation [3,21] based on the Budyko hypothesis [14] has been used for predicting the long-term average evapotranspiration and the interannual variability of evapotranspiration. The top-down approach is usually used for explaining the observed responses at the watershed scale, in which one problem is how to generalize the catchment hydrological pattern and whether the hypothesis of conceptualization is reasonable. Another problem is how to explain the interactions between the response at watershed scale and the processes that contributed to it that occur at smaller scales. The top-down approach has not been widely used in hydrological prediction, but as Sivapalan et al. [5] mentioned, this approach should become an important component of the toolkit for data analysis and hydrological model development.

The bottom-up approach in hydrology generally uses "process-based" or "physically based" distributed hydrological models, which can predict overall catchment's water balance components based on process simulation at smaller spatial and temporal scales. In order to understand the hydrological processes at a local scale and to analyze the temporal and spatial variability of water resources at a watershed scale, a number of distributed hydrological models have been developed: SHE model [22–25], IHDM model [26], SLURP model [27], SWAT model [28], GBHM model [29–32], WEP [33], VIC [34], etc. These and many other models have been developed and have been applied to interpret and predict the impacts of land-use change and climate variability. A bottom-up model requires great amounts of input data for describing variable rainfall and evapotranspiration fields, topography, vegetation, soil, and other land surface conditions and also needs dozens of parameters for the representation of hydrological processes. Therefore, in the one hand, the costs would be prohibitively high. Beven [35] discussed the problems of distributed model including the problem of nonlinearity, scale, equifinality, uniqueness, and uncertainty. Because the physically-based distributed hydrological models can offer both detailed information of hydrological processes inside a catchment and general catchment hydrological pattern, this kind of models are usually used to analyze the hydrological impacts of land use and climate changes.

Most recently there are discussions on the direction of hydrological study, which focus on either estimating predictive uncertainty or understanding catchment hydrological function [36–38]. For better understanding of catchment hydrology, we need a change in the methodology of hydrological analysis. Though both the bottom-up and the top-down approaches are widely used in catchment hydrology, few studies have been carried out on the linkage between these two methods. Klemes [4] first suggested the combination of these two approaches and mentioned that "the most promising route to significant new discoveries in hydrology is to combine the upward and downward research based on the existing facts and knowledge, as well as on imagination and intuition, to form testable hypotheses, i.e., to apply the time-honored scientific method." Sivapalan et al. [5] also anticipated that "in the near future, studies that address the same problem by both approaches at the same time will make a significant impact on a better understanding of hydrologic prediction issues." Based on the previous study, this paper attempts to build a connection between the top-down and the bottom-up approaches and to understand the dominant factors on catchment evapotranspiration at different time scales using distributed physically-based hydrological model and simple water-energy balance model.

2 Study area and data availability

The Luan River basin is located in the region delimited by geographical coordinates 40.4°N–42.6°N and 115.5°E–118.9°E with the elevation ranging about 150–2000 m above the sea level. The Panjiakou Reservoir is the largest reservoir on the Luan River in northern China. The upstream watershed of the Panjiakou Reservoir is selected as the study area in this study (see Fig. 1).

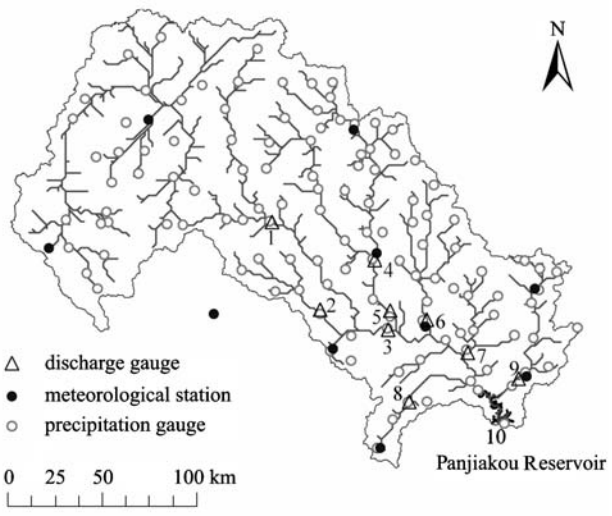

1: Guojiatun; 2: Boluonuo; 3: Sandaohezi; 4: Xiahenan; 5: Hanjiaying; 6: Chengde; 7: Xiabancheng; 8: Liying; 9: Kuancheng; 10: Panjiakou

Fig. 1 Study area

The catchment extent and topography are represented using the digital elevation model (DEM) of a 90 m

resolution, which is obtained from the global topography database (http://telascience.sdsc.edu/tela_data/SRTM/version2/SRTM3/). Land use map of 100 m resolution was from Data Center for Resources and Environmental Sciences of Chinese Academy of Sciences. Based on the available data, the land use has been regrouped into seven categories including water body, urban area, forest, irrigated cropland, upland, grassland, and shrub for the study area. Seasonal change of vegetation is expressed by the monthly leaf area index (LAI) derived from monthly NDVI (NDVI data is obtained from the DAAC website of GSFC/NASA: http://daac.gsfc.nasa.gov/DAAC_DOCS/). The soil type used here is obtained from the FAO-UNESCO's 1∶5 million scale Soil Map of the World [39]. The soil properties used for the hydrological simulation including the porosity, the saturated hydraulic conductivity, and the other soil water parameters corresponding to each soil type in this map are obtained from the Global Soil Data Task [40] with an 8-km resolution.

Daily meteorological data are obtained from the China Meteorological Administration and additional daily precipitation data are obtained from the Ministry of Water Resources of the People's Republic of China. The daily meteorological data consist of precipitation, temperature, average wind speed, relative humidity, sunshine duration, etc. There are 10 meteorological stations and 121 precipitation gauges in this region (see Fig. 1). From the two data sets, a time period from 1980 to 1991 is selected according to the availability of records in these meteorological stations and precipitation gauge. The gridded meteorological data required as input to the distributed hydrological model is interpolated from the gauge data. Precipitation is interpolated using an angular-distance weighting method [41]. In the same way, the wind speed, relative humidity, and sunshine hours are also interpolated into each grid. The temperatures (maximum, minimum, and mean) are interpolated using an elevation-corrected angular-direction weighting method. The daily potential evapotranspiration is calculated using the wind speed, relative humidity, sunshine hours, and temperature [42].

The discharge data are collected for the same period of 1980–1991 from the "Hydrological Year Book" published by the Hydrological Bureau of the Ministry of Water Resources of the People's Republic of China. In this study, seven gauges located on the tributaries (1: Guojiatun; 2: Boluonuo; 4: Xiahenan; 5: Hanjiaying; 6: Chengde; 7: Xiabancheng; 8: Liying) and two gauges (3: Sandaohezi; 9: Kuancheng) located on the mainstream (see Fig. 1) are selected for analysis.

3 Methodology

The ratio of evapotranspiration to precipitation in the study area is nearly 70%–80%; therefore, the estimation of evapotranspiration is important for understanding the catchment water balance. The physically-based hydrological model can estimate hourly evapotranspiration at hillslope scale, and through a bottom-up analysis, the hourly evapotranspiration in each hillslope can be integrated into daily, monthly, annual, and long-term mean annual evapotranspiration at catchment scale, which offers a reference for the top-down analysis. The long-term mean annual evapotranspiration of a catchment can be estimated using water-energy balance model first, and through top-down analysis, the temporal scale is downward to year, month, and day for identifying the dominant factors on catchment evapotranspiration at different time scales.

3.1 Distributed hydrological model—GBHM model

Since the GBHM model has been successfully applied in the Yellow River [31,32] and the Yangtze River [43,44], it is chosen as a bottom-up tool to simulate the hydrological processes and the evapotranspiration in the Luan River basin. As shown in Fig. 2, a 2-km grid is used for discretization of the study catchment, in which a subgrid parameterization scheme is employed to represent the hillslope topography [30]. The procedures of model construction contain catchment subdivision, subgrid parameterization, physically-based hydrological simulation on hillslope, and kinematic wave flow routing.

A total of 97 sub-catchments were divided for the study catchment. For each sub-catchment, the geomorphologic property of stream-hillslope formation is used for representing the catchment topography, and it is also assumed that a large grid is comprised of a set of hillslopes located along the streams. From a macroscale viewpoint, the hillslopes located in a grid are viewed as being geometrically similar. A hillslope with a unit width is called a hillslope element, represented by a rectangular inclined plane with slope of β and length of l (see Fig. 2).

Considering the land cover heterogeneity, hillslopes located in a 2-km grid are grouped. The soil within a grid is represented as a single dominant soil type. The runoff generated from one grid is the sum of surface and subsurface runoff. The vertical flux, the actual evapotranspiration, is the total evapotranspiration simulated from all of the hillslopes. The soil moisture content is taken as the area-averaged soil moisture of all the hillslopes.

The hydrological processes included in the GBHM model are snowmelt, canopy interception, evapotranspiration, infiltration, surface flow, subsurface flow, and the exchange between the groundwater and the river [29–31], which are simulated at a 1-hour time step. Actual evapotranspiration is estimated from potential evapotranspiration, which is calculated by the Penman equation [1]. Considering seasonal variation of LAI, root distribution, and soil moisture availability, it is computed individually from the canopy water storage, root zone, and soil surface. For each 1-hour time step, actual evaporation rate E_{canopy} from the canopy storage is expressed as

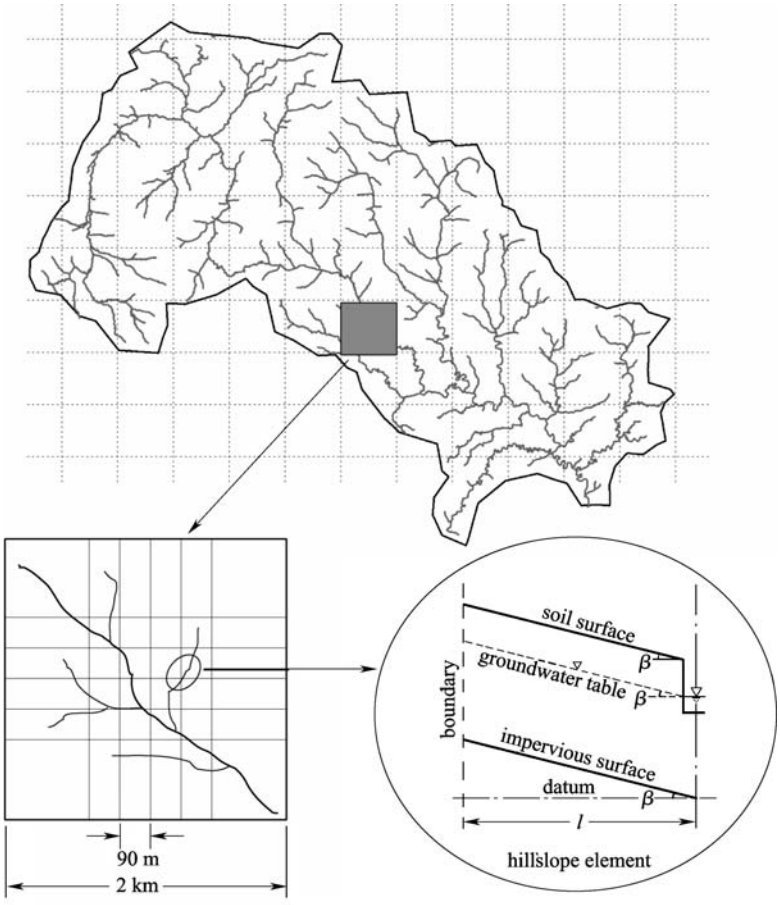

Fig. 2 Structure of the GBHM model

$$E_{\text{canopy}} = K_{\text{c}} E_{\text{p}}, \tag{1}$$

where E_{p} is the potential evaporation rate, and K_{c} is the crop coefficient. The vegetation transpiration rate is estimated as the rate of water taken up from the root zone and follows the equation

$$E_{\text{tr}}(z_j) = K_{\text{c}} E_{\text{p}} f_1(z_j) f_2(\theta_j) \frac{\text{LAI}}{\text{LAI}_0}, \tag{2}$$

where $E_{\text{tr}}(z_j)$ is the transpiration rate from the layer j of root zone; $f_1(z_j)$ is the root distribution function that is given by a triangular distribution with its maximum near the surface; $f_2(\theta_j)$ is given as a linear function of soil moisture θ_j; and LAI_0 is the maximum leaf area index of the vegetation in a year. For the bare soil, the evaporation rate is given by

$$E_{\text{s}} = K_{\text{c}} E_{\text{p}} f_2(\theta), \tag{3}$$

where E_{s} is the evaporation rate from the soil surface. In ponding conditions, the value of $f_2(\theta)$ is 1. The actual transpiration from the root zone and the evaporation from the soil surface are treated as sink terms in Richards' equation that is employed to model soil water movement in unsaturated zone.

Infiltration and subsurface flow in the vertical direction and along the hillslope are described in a quasi-two-dimensional subsurface model. The vertical water flow in the topsoil is represented by the Richards' equation. The soil water distribution along the hillslope is treated as uniform. When the soil water content in each layer is more than the field capacity, water moves to the stream along the hillslope by gravity.

The surface runoff, from the infiltration excess and saturation excess, is obtained by solving the Richards' equation and flows to the river along the hillslope by a kinematic wave. The groundwater aquifer is treated as an individual storage corresponding to each grid. The exchange between the groundwater and the river water is considered as steady flow and is calculated by the Darcy's law [30]. The runoff generated from the grid is the lateral inflow into the river at the same flow interval. Flow routing in the river network is solved using the kinematic wave approach.

The parameters used in the model include vegetation parameters, land surface parameters, soil-water properties, river parameters, a snow-melting parameter, and a groundwater parameter. Since most parameters have their physical

meanings, they can be estimated through field tests. This study specifies the parameters by referring to the existing database and handbooks. A six-year test run from 1980 to 1985 is carried out for calibrating the model parameters. One of the calibrated parameters in this model is the snowmelt factor in the temperature-based snowmelt equation. Another calibrated parameter, the hydraulic conductivity of the groundwater, is calibrated by checking the base flow in different sub-basins. Model validation is carried out from 1986 to 1991. In the calibration period, the Nash-Sutcliffe coefficient R^2 for the simulated daily discharges at the outlet of the study area is nearly 0.80, and the absolute values of the relative error RE are less than 2%. For the major tributaries, the values of R^2 are larger than 0.65, and the absolute values of the relative error RE are less than 8% and the others are more than 10%. This showed that hydrological simulation by the GBHM model is reasonable.

3.2 Water-energy balance model

Evapotranspiration is the key component linking water balance with energy balance. The primary factors controlling the long-term mean evapotranspiration are the local interaction of water supply (precipitation) and demand (potential evapotranspiration). Budyko [14] assumed that actual evapotranspiration is controlled by both water and energy availabilities and considered that the ratio of annual evapotranspiration and annual precipitation is the function of the ratio of annual precipitation and annual net radiation. Based on the Budyko hypothesis and based on dimensional analysis and mathematical reasoning, Yang et al. [20] considered the important effect of the vegetation and derived an analytical equation of the coupled water-energy balance at an annual time scale, expressed as

$$E = \frac{E_0 P}{(P^n + E_0^n)^{1/n}}, \tag{4}$$

where P is the precipitation, and the parameter n represents the effect of the catchment landscape characteristics, such as vegetation, soil properties, and slope gradient. This theoretical equation has also been extended to a variety of time scales.

In order to consider the effect of the vegetation, Yang et al. [45] changed the relative soil water storage $S_{\max}/E_0$ in the parameter ϖ to vegetation coverage M in the parameter n. The empirical formula of parameter n is given for the Haihe River basin as

$$n = 2.721\left(\frac{K_s}{\overline{i}_r}\right)^{-0.393} M^{-0.301}\exp\left(4.351\tan\overline{\beta}\right), \tag{5}$$

where $K_s/\overline{i}_r$ is the relative infiltration capacity defined as the ratio of saturated hydraulic conductivity K_s to mean precipitation intensity $\overline{i}_r$, $\overline{\beta}$ is the average slope, and the monthly vegetation coverage M was calculated from the NDVI data by using the method proposed by Gutman and Ignatov [46]:

$$M = (\mathrm{NDVI} - \mathrm{NDVI}_{\min})/(\mathrm{NDVI}_{\max} - \mathrm{NDVI}_{\min}). \tag{6}$$

The actual evapotranspiration obtained from Eqs. (4) and (5) showed remarkable agreement with that derived from the long-term water balance at Haihe River basin [45,47], so Eqs. (4) and (5) were used in this study to calculate the actual annual evapotranspiration. In order to validate the water-energy balance model given by Eqs. (4) and (5) at annual time scale, the actual annual evapotranspiration simulated for each sub-catchment were plotted against the actual annual evapotranspiration estimated from the observed precipitation subtracting the observed runoff by neglecting the change of water storage (see Fig. 3). Most values of predicted annual evapotranspiration are much close to the observed ones, which shows good simulation of annual evapotranspiration. The relative error between the long-term average evapotranspiration calculated by this model and the actual evapotranspiration estimated from the long-term water balance is less than 5%.

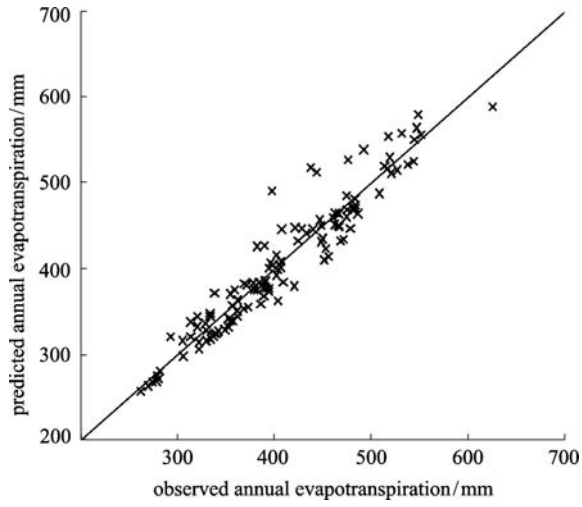

Fig. 3 Predicted value of annual evapotranspiration by water-energy balance model plotting versus observed one (the 1:1 line is plotted for comparison)

As Eq. (4) does not consider interannual variability of soil water content, Yang et al. [48] derived another equation to estimate the evapotranspiration at arbitrary time scale, which contains the variability of soil water, followed as

$$E = E_0(P + S)/((P + S)^n + E_0^n)^{1/n}, \tag{7}$$

in which S is the initial soil water of each simulation time period (i.e., annual, monthly, and daily period).

To use the above equation for continuous simulation, we rewrite Eq. (7) as

$$E_i = E_{0,i}(P_i + S_{i-1})/((P_i + S_{i-1})^n + E_{0,i}^n)^{1/n}, \quad (8)$$

in which i represents the ith simulation time period, and S_{i-1} represents the initial soil water content at the ith period. Moreover, the soil water content at the end of the ith period can be derived from the water balance equation as

$$S_i = P_i + G_i - R_i - E_i + S_{i-1}, \quad (9)$$

in which G_i is the groundwater recharge. The value of G_i is ignored since it is the relatively small value in the study area.

The evapotranspiration at arbitrary time scales can be simulated using Eqs. (8) and (9) as long as the initial soil water content S_0 is given. The value of S_0 is derived from the continuous simulation at the first several simulation periods. The parameter n in Eq. (8) is calculated at different time scale according to Eq. (5); however, at the daily time scale, the same parameter as the monthly scale is used due to the vegetation data availability.

4 Results and discussion

4.1 Bottom-up analysis

The GBHM model used a linear assumption at hourly temporal and hillslope spatial scale, that is, the actual evapotranspiration for a hydrological unit at hourly scale is estimated to be proportional to the potential evapotranspiration (see Eqs. (1)–(3)). It is known that annual precipitation, potential, and actual evapotranspiration are following the Budyko curve at catchment scale. Based the long-term evapotranspiration estimated by GBHM, Fig. 4 plots the annual precipitation, potential, and actual evapotranspiration for the nine sub-catchments and the whole watershed in two alternative forms of the Budyko curves, i.e., E/P vs E_0/P and E/E_0 vs P/E_0. The value of parameter ϖ ranges from 2.5 to 2.95 in the study area, and all the points stand inside the two curves.

According to Yang et al.'s study [21], the actual evapotranspiration at annual and catchment scale is mainly controlled by precipitation rather than potential evapotranspiration in the nonhumid regions of China, and the relationship between the actual and potential evapotranspiration should be complementary. The actual and potential evapotranspiration is usually plotted against the precipitation for validating the complementary relationship of evapotranspiration. Figure 5 shows the complementary relationship between the actual and potential evapotranspiration, in which the actual evapotranspiration is simulated by the GBHM. In Figs. 4 and 5, it is known that annual catchment evapotranspiration simulated by the GBHM agrees with the Budyko curve and followed the complementary relationship with potential evapotranspiration, which shows that the GBHM could simulate interaction between the land surface and atmosphere.

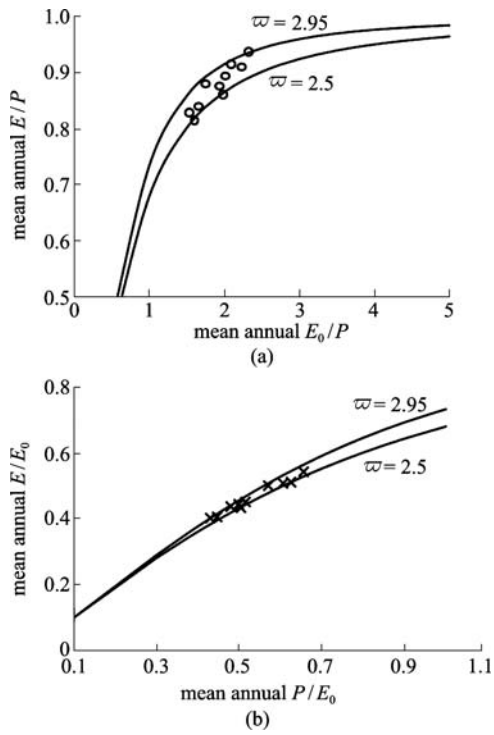

Fig. 4 Long-term mean values of annual actual evapotranspiration (E), precipitation (P), and potential evapotranspiration (E_0) for the nine sub-catchments and the whole catchment are plotted in two different, but equivalent Budyko-type forms (plotted in scattering points) together with the Budyko curves with the regional average values of parameter ϖ. (a) E/P vs E_0/P; (b) E/E_0 vs P/E_0

For a general case, the actual evapotranspiration is determined mainly by the potential evapotranspiration, soil moisture, and vegetation status, which can be expressed in a general form as $E = f(E_0, \theta, \text{vegetation})$ (θ is soil moisture content). This is an unknown nonlinear equation for the most cases in a real catchment. One analytical solution of this equation is given as Eq. (4), which shows a nonlinear relationship between the annual precipitation, potential, and actual evapotranspiration. This equation can also be calculated as the summation of the actual evapotranspiration at each 1-hour time step over the same year. At hourly time scale over a uniform landscape condition, the soil moisture can be viewed as constant and expressed as a soil moisture-impact factor (that is expressed as a stage-linear function of soil moisture content) in the equation; and the leaf-area-index can also viewed as constant and expressed as a vegetation-impact factor. Therefore, the linear assumption (see Eqs. (1)–(3)) for a hydrological unit with relative uniform landscape condition at a short time scale (1-hour in this model) can be adopted.

The complementary relationship between the actual and potential evapotranspiration results from the interaction between the land surface and atmosphere. For a given net radiation, a decrease in actual evapotranspiration will cause an increase in sensible heat flux and then an increase

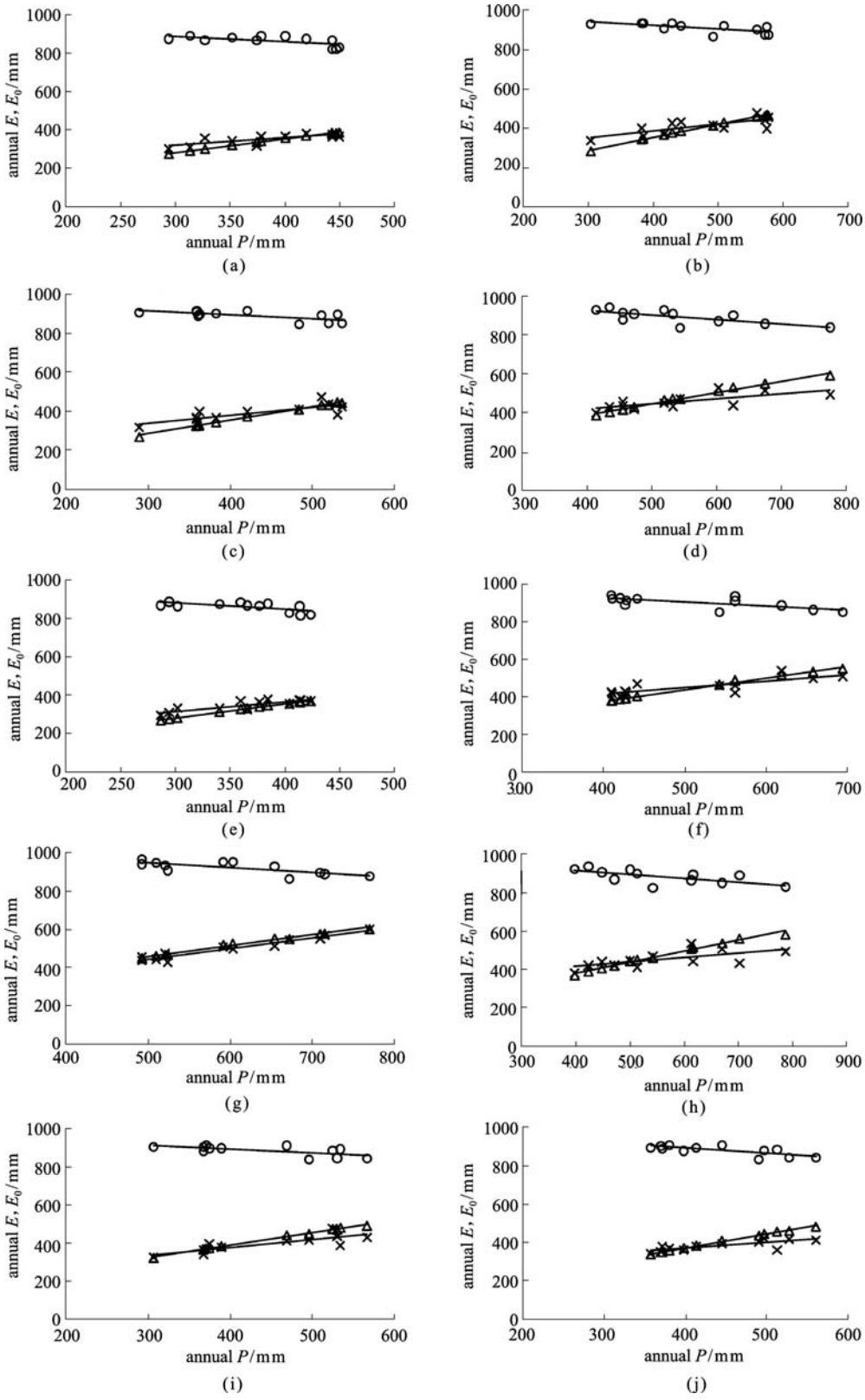

Fig. 5 Relationship between annual values of actual evapotranspiration (E) and potential evapotranspiration (E_0) plotted versus annual precipitation (P). (a)–(i) represent No. 1–9 sub-catchments, respectively, and (j) represents the whole study catchment. (The circular dots represent potential evapotranspiration (E_0), the cross dots represent actual annual evapotranspiration (E) predicted by GBHM, and the triangular dots represent actual annual evapotranspiration (E) predicted by water-energy balance model.)

in potential evapotranspiration due to the land surface-atmosphere interactions [49]. Budyko [14] assumed that actual evapotranspiration is controlled by both water and energy availabilities. At the annual time scale, the water availability is the amount of annual precipitation and the energy availability can be measured by the potential evapotranspiration. The water-energy balance given by Eq. (4) describes the nonlinear relationship among annual precipitation, potential, and actual evapotranspiration and the land surface-atmosphere interactions. In the GBHM, the potential evapotranspiration rate E_0 is estimated using Penman's equation based on the daily meteorological data, which is the synthesized result of net radiation and turbulent diffusion including the feedback from land surface (e.g., the vapor pressure and air temperature are affected by the land surface evapotranspiration). Therefore, the actual evapotranspiration simulated by the GBHM model also includes the interaction and feedback between land surface and atmosphere.

4.2 Top-down analysis

A lumped water-energy balance model is used in the top-down analysis for understanding the major controlling factors of the evapotranspiration at different temporal scales. The actual evapotranspiration simulated by the GBHM was used as a reference for this analysis. Analysis is from a long-term time scale down to an annual, monthly, and daily time scale. At the long-term time scale, Eq. (4) is used to estimate the actual evapotranspiration; at the annual time scale, Eq. (4) is used to estimate the actual evapotranspiration neglecting the interannual variability of soil moisture; at the monthly and daily time scale, Eq. (8) is used with consideration of the soil moisture availability.

1) Actual evapotranspiration at long-term time scale

The mean annual evapotranspiration is controlled by the local interaction of fluctuating water supply (precipitation) and demand (potential evapotranspiration) at long-term time scale. Figure 6 and Table 1 show the comparison of the long-term mean values of actual evapotranspiration estimated from the annual precipitation and runoff data by neglecting the change of water storage, simulated by the GBHM model, and the water-energy balance model. It can be seen that the values of the actual evapotranspiration by different models are in a good agreement. Considering the value estimated from the long-term water balance by neglecting the change of water storage as the "true value" (which is denoted as the "observation"), the relative error for the simulated annual evapotranspiration are within ±5% by both the GBHM and water-energy balance model.

2) Actual evapotranspiration at annual time scale

In order to understand interannual variability and the major controlling factors of catchment evapotranspiration at annual time scale, assuming vegetation condition is unchangeable or changeable and neglecting or considering the variability of soil water, four different conditions are used in the simulation for comparison: 1) using Eq. (4) with the same value of parameter n for every year in each

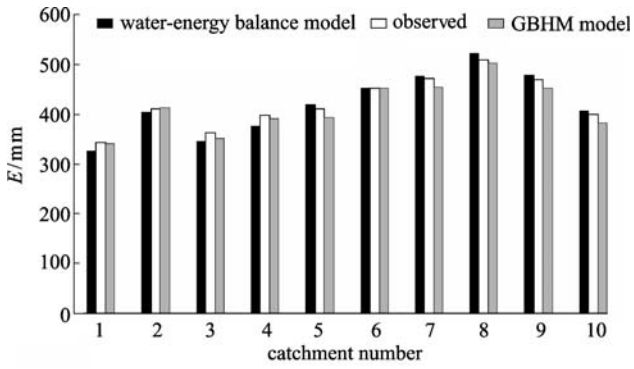

Fig. 6 Comparison of long-term average evapotranspiration estimated by water-energy balance model, GBHM model and from the observed data (No. 1–9 represents the nine sub-catchments, and No. 10 represents the whole watershed)

Table 1 Comparison of long-term water balance simulated by the GBHM and water-energy balance model

No.	gauges	river	P/mm	R/mm	E/mm			RE/%	
					E_{wb}	E_{webm}	E_{gbhm}	RE_1	RE_2
1	Guojiatun	Luan River	356.8	21.7	335.1	319.3	340.7	−4.72	1.67
2	Boluonuo	Xingzhou River	453.1	59.8	393.2	393.3	411.5	0.00	4.63
3	Sandaohezi	Luan River	375.5	23.8	351.7	336.6	351.5	−4.29	−0.07
4	Xiahenan	Yimatu River	420.7	29.8	390.9	372.5	389.7	−4.72	−0.32
5	Hanjiaying	Yixun River	426.8	30.0	396.7	409.5	393.7	3.21	−0.77
6	Chengde	Wulie River	503.4	62.1	441.2	444.2	452.3	0.69	2.51
7	Xiabancheng	Laoniu River	524.2	71.1	453.2	463.4	454.9	2.27	0.37
8	Liying	Liu River	595.3	96.6	498.6	516.0	501.0	3.47	0.47
9	Kuancheng	Pu River	533.5	85.7	447.7	464.4	452.5	3.72	1.07
10	Panjiakou	Luan River	430.0	45.2	384.8	395.1	381.8	2.68	−0.76

Notes: E_{wb}, E_{webm}, and E_{gbhm} represent mean values of actual evapotranspiration calculated by long-term water balance, the water-energy balance model, and the GBHM model, respectively; RE_1 and RE_2 are the relative errors of long-term mean values of actual evapotranspiration calculated using the water-energy balance model and the GBHM model, respectively, comparing with the value estimated by long-term water balance.

sub-catchment (denoted as Sim-A1), 2) using Eq. (4) with the different value of parameter n estimated using Eq. (5) according to the vegetation coverage for every year in each sub-catchment (denoted as Sim-A2), 3) using Eq. (8) with the same value of parameter n for every year in each sub-catchment(denoted as Sim-A3), and 4) using Eq. (8) with the different value of parameter n estimated using Eq. (5) according to the vegetation coverage for every year in each sub-catchment (denoted as Sim-A4). Taking average values of the annual evapotranspiration during the simulated period (1980–1991) for each sub-catchment simulated by the water-energy balance model and comparing with the observation, Table 2 shows the relative error. The results show that Sim-A3 and Sim-A4 have a better result than Sim-A1 and Sim-A2, which implies that it is essential to consider the interannual variability of soil moisture for estimating annual catchment evapotranspiration. Table 2 also shows that catchment annual evapotranspiration is more sensitive to the soil water than to the vegetation coverage. Figure 7 shows the interannual variability of the actual evapotranspiration in each sub-catchment from 1980 to 1991 simulated by the water-energy balance model in Sim-A4 (considering interannual variability of both vegetation and soil water) and the GBHM model. It can be seen that both results have a very similar temporal pattern for the 10 sub-catchments. The results show that both the simple lumped water-energy balance model and the physically-based distributed hydrological model can predict catchment annual evapotranspiration and its interannual variability.

3) Actual evapotranspiration at monthly time scale

At monthly time scale, similar assumptions and similar four conditions as the above were used in the simulation of monthly evapotranspiration, i.e., 1) using Eq. (4) with a constant parameter n for each sub-catchment (denoted as Sim-M1), 2) using Eq. (4) with the different value of parameter n for every month in each sub-catchment (denoted as Sim-M2), (3) using Eq. (8) with a constant parameter n in each sub-catchment (denoted as Sim-M3), and 4) using Eq. (8) with the different value of parameter n for every month in each sub-catchment (denoted as Sim-M4). Monthly evapotranspiration are integrated to the long-term annual evapotranspiration, which is used to compare with the observation. Table 3 shows the results of the relative error for each sub-catchment. It can be seen that the result of Sim-M4 has the least relative error, which implies that it is essential to include variability of both soil water and vegetation coverage for estimating catchment evapotranspiration at monthly time scale. The results also indicate that the soil water content is more important than the parameter n for estimating the monthly evapotranspiration. Taking the whole study area as an example, Fig. 8 shows the comparison of the monthly evapotranspiration estimated by Sim-M4 of the water-energy balance model and by the GBHM model. Both results have a similar temporal pattern, but the highest and lowest peaks estimated by the water-energy balance model are larger/smaller than the peaks calculated by the GBHM model. In Eq. (8), the soil is considered as a single storage with no interaction with the groundwater, and this simplification may be a reason for the error shown in Fig. 8.

4) Actual evapotranspiration at daily time scale

Since the monthly NDVI data was used in the study, the parameter n only can be obtained at monthly time scale, and the daily parameter n is considered as the same in each month. At daily time scale, two different conditions are used: 1) neglecting the variability of soil water, which is using Eq. (4) (denoted as Sim-D1) with monthly parameter n; and 2) considering the variability of soil water, which is using Eq. (8) (denoted as Sim-D2) with monthly parameter n. Daily evapotranspiration is integrated into the long-term mean value of annual evapotranspiration for comparing with the observation. Table 4 shows the relative error for each sub-catchment. It is clear that the result of Sim-D2 is much better than the result of Sim-D1, which implies that

Table 2 Annual evapotranspiration simulated by water-energy balance model with consideration of different soil water storage and vegetation

No.	gauges	RE/%			
		Sim-A1	Sim-A2	Sim-A3	Sim-A4
1	Guojiatun	−5.17	−7.71	−1.32	−2.60
2	Boluonuo	−8.11	4.39	−4.02	4.20
3	Sandaohezi	−7.30	−7.62	−2.42	−2.64
4	Xiahenan	−5.28	−1.44	−2.11	−0.28
5	Hanjiaying	−7.66	−1.81	−3.88	−0.29
6	Chengde	−5.59	4.78	−2.04	4.42
7	Xiabancheng	−7.93	5.22	−4.57	4.80
8	Liying	2.32	2.77	2.76	3.05
9	Kuancheng	2.25	2.90	2.38	2.71
10	Panjiakou	−2.73	−1.11	−0.33	0.11

Notes: Sim-A1, Sim-A2, Sim-A3, Sim-A4 represent four conditions in simulation of the annual evapotranspiration, i.e., Sim-A1: neglecting the change of the vegetation and soil water; Sim-A2: neglecting the change of soil water; Sim-A3: neglecting the change of the vegetation; Sim-A4: considering the change of the vegetation and soil water. RE is the relative errors of the mean values of annual actual evapotranspiration calculated using the water-energy balance model.

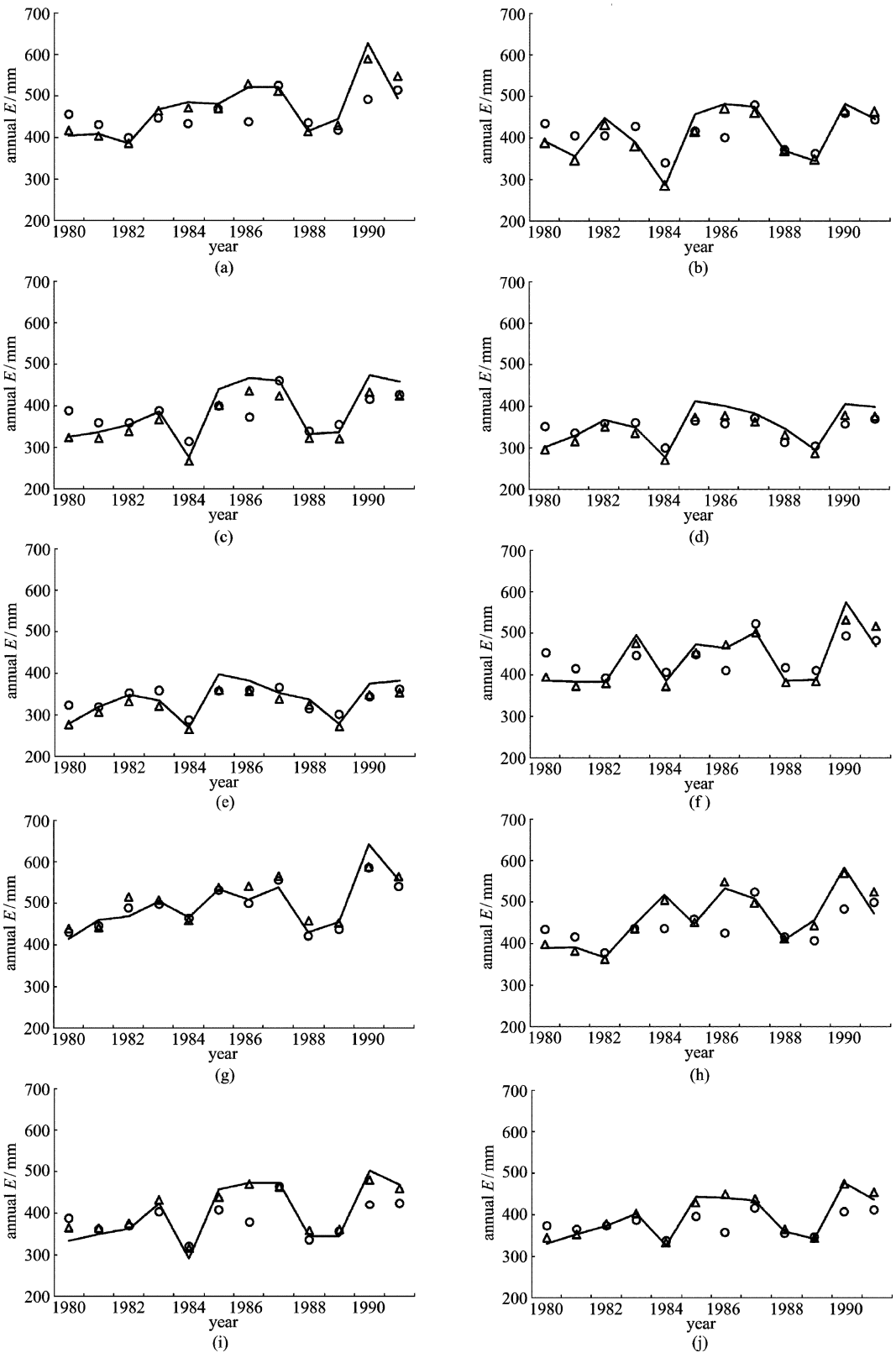

Fig. 7 Comparison of annual evapotranspiration estimated by the water-energy balance model and GBHM model and the observed one. (a)–(i) represent No. 1–9 sub-catchments, respectively; (j) represents the whole watershed. (The real lines represent observed annual evapotranspiration (E), the circular dots represent actual annual evapotranspiration (E) predicted by GBHM, and the triangular dots represent actual annual evapotranspiration (E) predicted by the water-energy balance model.)

Table 3 Monthly evapotranspiration simulated by the water-energy balance model with consideration of different soil water storage and vegetation

No.	gauges	RE/%			
		Sim-M1	Sim-M2	Sim-M3	Sim-M4
1	Guojiatun	−19.88	−18.11	−2.39	−1.14
2	Boluonuo	−16.32	−13.24	−2.51	−0.26
3	Sandaohezi	−20.07	−17.72	−4.53	−2.47
4	Xiahenan	−16.31	−13.90	−5.03	−2.67
5	Hanjiaying	−17.30	−15.10	−7.71	−5.52
6	Chengde	−13.33	−11.22	−8.29	−5.89
7	Xiabancheng	−15.94	−13.83	−3.07	−2.01
8	Liying	−14.10	−8.22	−4.44	−1.82
9	Kuancheng	−12.61	−10.59	−5.29	−3.29
10	Panjiakou	−15.38	−12.77	−4.86	−2.68

Notes: Sim-M1, Sim-M2, Sim-M3, and Sim-M4 represent four conditions in simulation the monthly evapotranspiration, i.e., Sim-M1: neglecting the change of the vegetation and soil water; Sim-M2: neglecting the change of soil water; Sim-M3: neglecting the change of the vegetation; and Sim-M4: considering the change of the vegetation and soil water. RE is the relative errors of the mean values of annual actual evapotranspiration calculated using the water-energy balance model.

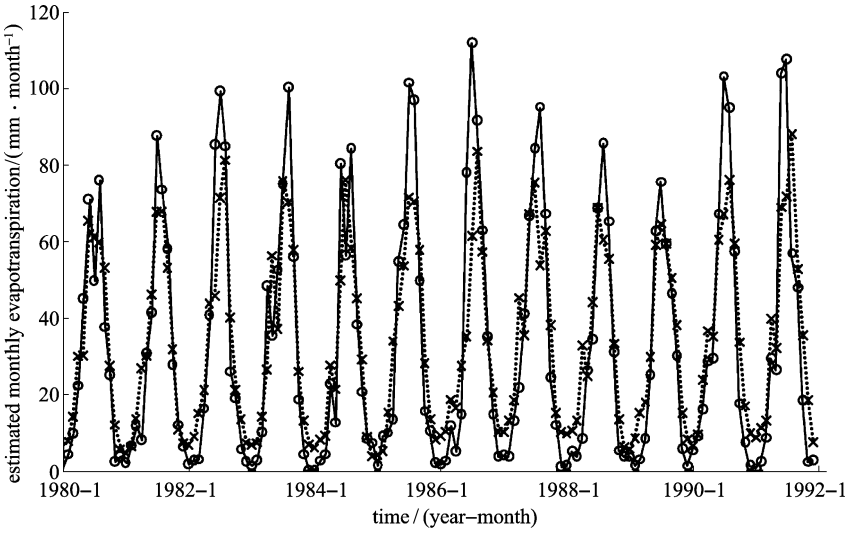

Fig. 8 Comparison of monthly evapotranspiration estimated by the water-energy balance model and GBHM model for the whole watershed (The circular real line represents the actual monthly evapotranspiration (*E*) predicted by water-energy balance model, and the cross dashed line represents the actual monthly evapotranspiration (*E*) predicted by GBHM)

the soil water content is a very important factor controlling the daily evapotranspiration. Comparing the results simulated at daily time scale by the water-energy balance model and by the GBHM model for the whole study area, it can be seen that the simple water-energy balance model is not possible to simulate the daily variability of evapotranspiration without consideration of the soil moisture storage. However, with consideration of the soil water storage, this simple model is also difficult to capture the daily variability appropriately. As it is known that soil water movement usually cannot penetrate the whole soil layer (e.g., 1-m depth) within a day, therefore, it is important to describe the soil water dynamics at daily or shorter time scale rather than to consider a total storage of the soil water.

5 Conclusions

In this study, the bottom-up and top-down analysis based on the GBHM model and the simple water-energy balance model derived from Budyko hypothesis was carried out for understanding the dominant factors on catchment evapotranspiration at different scales in nine sub-cachments and the whole basin of the Luan River in northern China. In annual and long-term time scales, a consistent result has been achieved by the two models, which show the complementary relationship between the actual and potential evapotranspiration at annual time scale for the study areas. However, at a shorter time scale, the difference between the two simulations by GBHM and the water-energy balance model became larger. On the basis of

Table 4 Daily evapotranspiration simulated by the water-energy balance model with consideration of different soil water storage

No.	gauges	RE/%	
		Sim-D1	Sim-D2
1	Guojiatun	−41.73	−2.55
2	Boluonuo	−46.73	−5.25
3	Sandaohezi	−41.05	−2.84
4	Xiahenan	−43.15	−6.55
5	Hanjiaying	−42.85	−7.55
6	Chengde	−44.81	−8.68
7	Xiabancheng	−48.31	−11.56
8	Liying	−50.15	−14.30
9	Kuancheng	−49.54	−8.16
10	Panjiakou	−37.90	−1.32

Notes: Sim-D1 and Sim-D2 represent two conditions in simulation the daily evapotranspiration, i.e., Sim-D1: neglecting the change soil water; Sim-D2: considering the change of soil water. RE is the relative errors of the mean values of annual actual evapotranspiration calculated using the water-energy balance model.

comprehensive intercomparison in the framework of the top-down and bottom-up analysis through different temporal scales, it can be concluded as follows:

1) The annual catchment water balance pattern can be predicted successfully by both the simple lumped model and the detailed distributed model in the study areas.

2) The relationships between potential and actual evapotranspiration can be different at different temporal and spatial scales. It shows highly nonlinear relationship at annual and catchment scale but can be simplified as a linear relationship at hourly and hillslope scale.

3) The soil water storage and the soil water dynamics become more important for simulation of evapotranspiration at a shorter temporal scale.

4) Consideration of vegetation coverage can improve the simulation of interannual and seasonal variability of catchment evapotranspiration in the lumped water-energy balance model.

5) Comparison of the top-down and the bottom-up methods can offer a new way for understanding the catchment hydrological behavior at different temporal and spatial scales and is potentially helpful for developing new generation of hydrological model.

Acknowledgements The authors would like to express their appreciation to Professor Murugesu Sivapalan for his helpful comments and suggestions during the manuscript preparation. The research was supported by the National Key Technology R&D Program of China (No. 2006BAB14B02-01) and by the Ministry of Water Resources of the People's Republic of China (Contract No. 20081012).

References

1. Penman H L. Natural evaporation from open water, bare and grass. Proceedings of the Royal Society of London, Series A, 1948, 193: 120–145
2. Allen R G, Pereira L S, Raes D, Smith M, eds. Crop Evapotranspiration: Guidelines for Computing Crop Water Requirements. FAO Irrigation and Drainage Paper 56. Rome: Food and Agriculture Organization of the United Nations, 1998
3. Yang D, Sun F, Liu Z, Cong Z, Ni G, Lei Z. Analyzing spatial and temporal variability of annual water-energy balance in non-humid regions of China using the Budyko hypothesis. Water Resource Research, 2007, 43: W04426, doi: 10.1029/2006WR005224
4. Klemes V. Conceptualization and scale in hydrology. Journal of Hydrology, 1983, 65(1–3): 1–23
5. Sivapalan M, Blöschl G, Zhang L, Vertessy R. Downward approach to hydrological prediction. Hydrological Processes, 2003, 17(11): 2101–2111
6. Littlewood I G, Croke B F W, Jakeman A J, Sivapalan M. The role of 'top-down' modelling for prediction in Ungauged Basins (PUB). Hydrological Processes, 2003, 17(8): 1673–1679
7. Jothityangkoon C, Sivapalan M, Farmer D. Process controls of water balance variability in a large semi-arid catchment: Downward approach to hydrological model development. Journal of Hydrology, 2001, 254(1–4): 174–198
8. Atkinson S, Sivapalan M, Woods R A, Viney N R. Dominant physical controls of hourly streamflow predictions and an examination of the role of spatial variability: Mahurangi catchment, New Zealand. Advances in Water Resources, 2002, 26(2): 219–235
9. Atkinson S, Sivapalan M, Viney N R, Woods R A. Physical controls of space-time variability of hourly streamflows and the role of climate seasonality: Mahurangi catchment, New Zealand. Hydrological Processes, 2003,17: 2171–2193
10. Farmer D, Sivapalan M, Jothityangkoon C. Climate, soil, and vegetation controls upon the variability of water balance in temperate and semiarid landscapes: Downward approach to water balance analysis. Water Resource Research, 2003, 39(2): 1035, doi: 10.1029/2001WR000328
11. Eder G, Sivapalan M, Nachtnebel H P. Modeling of water balances in Alpine catchment through exploitation of emergent properties over changing time scales. Hydrological Processes, 2003, 17 (11): 2125–2149
12. Son K, Sivapalan M. Improving model structure and reducing parameter uncertainty in conceptual water balance models through the use of auxiliary data. Water Resource Research, 2007, 43: W01415, doi: 10.1029/2006WR005032
13. Zhang L, Potter N, Hickel K, Zhang Y Q, Shao Q X. Water balance modeling over variable time scales based on the Budyko framework—Model development and testing. Journal of Hydrology, 2008, 360(1–4): 117–131
14. Budyko M I, ed. Climate and Life. translated from Russian by Miller D H. San Diego, CA: Academic, 1974
15. Fu Baopu. On the calculation of the evaporation from land surface. Scientia Atmospherica Sinica, 1981, 5(1): 23–31 (in Chinese)
16. Milly P C D. Climate, soil water storage, and the average annual water balance. Water Resource Research, 1994, 30: 2143–2156
17. Choudhury B J. Evaluation of an empirical equation for annual evaporation using field observations and results from a biophysical model. Journal of Hydrology, 1999, 216(1–2): 99–110
18. Wolock D M, McCabe G J. Explaining spatial variability in mean

annual runoff in the conterminous United States. Climate Research, 1999, 11: 149–159

19. Zhang L, Hickel K, Dawes W R, Chiew F H S, Western A W, Briggs P R. A rational function approach for estimating mean annual evapotranspiration. Water Resource Research, 2004, 40: W02502, doi: 10.1029/2003WR002710
20. Yang H, Yang D, Lei Z, Sun F. New analytical derivation of the mean annual water-energy balance equation. Water Resource Research, 2008, 44: W03410, doi: 10.1029/2007WR006135
21. Yang D, Sun F, Liu Z, Cong Z, Lei Z. Interpreting the complementary relationship in non-humid environments based on the Budyko and Penman hypotheses. Geophysical Research Letters, 2006, 33: L18402, doi: 10.1029/2006GL027657
22. Beven K J, Warren R, Zaoui J. SHE: towards a methodology for physically-based, distributed forecasting in hydrology. In: Hydrological forecasting, Proceedings of the Oxford Symposium, IAHS-AISH Publication No. 129. Wallingford, UK: AISH Publication, 1980, 133–137
23. Abbott M B, Bathurst J C, Cunge J A, O'Connell P E, Rasmussen J. An introduction to the European Hydrological System-Systeme Hydrologique Europeen. "SHE", 1: History and philosophy of a physically-based, distributed modelling system. Journal of Hydrology, 1986, 87(1–2): 45–59
24. Bathurst J C, Wicks J M, O'Connell P E. The SHE/SHESED basin scale water flow and sediment transport modeling system. In: Singh V P, ed. Computer Models of Watershed Hydrology. Littleton, CO: Water Resources Publications, 1995, 563–594
25. Refsgaard J C, Storm B. MIKE SHE. In: Singh V P, ed. Computer Models of Watershed Hydrology. Highlands, CO: Water Resources Publications, 1995, 809–846
26. Morris E M. Forecasting flood flows in grassy and forested basins using a deterministic distributed mathematical model. In: Hydrological forecasting, Proceedings of the Oxford Symposium, IAHS-AISH Publication No. 129. Wallingford, UK: AISH Publication, 1980, 247–265
27. Kite G W. The SLURP model. In: Singh V P, ed. Computer Models of Watershed Hydrology. Highlands, CO: Water Resources Publications, 1995
28. Arnold J G, Srinivasan R, Muttiah R S, Williams J R. Large area hydrologic modelling and assessment part I: model development. Journal of the American Water Resources Association, 1998, 34 (1): 73–89
29. Yang D, Herath S, Musiake K. Development of a geomorphology-based hydrological model for large catchments. Annual Journal of Hydraulic Engineering, JSCE, 1998, 42: 169–174
30. Yang D, Oki T, Herath S, Musiake K. A geomorphology-based hydrological model and its applications. In: Singh V P, Frevert D K, eds. Mathematical Models of Small Watershed Hydrology and Applications. Littleton, CO: Water Resources Publications, 2002, 259–300
31. Yang D, Li C, Hu H, Lei Z, Yang S, Kusuda T, Koike T, Musiake K. Analysis of water resources variability in the Yellow River of China during the last half century using historical data. Water Resource Research, 2004, 40: W06502, doi: 10.1029/2003WR002763
32. Cong Z, Yang D, Gao B, Yang H, Hu H. Hydrological trend analysis in the Yellow River basin using a distributed hydrological model. Water Resource Research, 2009, 45, doi: 10.1029/2008WR006852
33. Jia Y W, Ni G H, Kawahara Y, Suetsugi T. Development of WEP model and its application to an urban watershed. Hydrological Processes, 2001,15(11): 2175–2194
34. Liang X. A two-layer variable infiltration capacity land surface representation for general circulation models. Washington DC: University of Washington, 1994
35. Beven K J. How far can we go in distributed hydrological modelling? Hydrology and Earth System Sciences, 2001, 5(1): 1–12
36. Beven K. On undermining the science? Hydrological Processes, 2006, 20: 3141–3146
37. Sivakumar B. Undermining the science or undermining Nature? Hydrologial Processes, 2008, 22(6): 893–897
38. Sivapalan M. The secret to 'doing better hydrological science': change the question! Hydrological Processes, 2009, 23(9): 1391–1396
39. FAO. FAO Map of World Soil Resources. Rome: Food and Agriculture Organization of the United Nations, 2003
40. IGBP-DIS (Global Soil Data Task: Global Soil Data Products CD-ROM). International Geosphere-Biosphere Programme- Data and Information Services. Available online at (http://www.daac.ornl.gov/) from the ORNL Distributed Active Archive Center, Oak Ridge National Laboratory, Oak Ridge, Tennessee, USA, 2000
41. New M, Hulme M, Jones P. Representing twentieth-century space-time climate variability. Part II: Development of a 1961-96 monthly grids of terrestrial surface climate. Journal of Climate, 2000, 13: 2217–2238
42. Shuttleworth W J. Evaporation. In: Maidment D R, ed. Handbook of Hydrology. New York: McGraw-Hill, 1993, 4.1–4.53
43. Xu Jijun, Yang Dawen, Ding Jinhua, Lei Zhidong. Development of space-nested watershed hydrological model and its application to floods forecasting of Three Gorges reservoir. Journal of Hydraulic Engineering, 2007, S1: 365–371 (in Chinese)
44. Xu J, Yang D, Lei Z, Chen J, Yang W. Spatial and temporal variation of runoff in the Yangtze River basin during the past 40 years. Quaternary International, 2008, 186(1): 32–42
45. Yang D, Shao W, Yeh P J-F, Yang H, Kanae S, Oki T. Impact of vegetation coverage on regional water balance in the non-humid regions of China. Water Resource Resaerch, 2009, 45: W00A14, doi: 10.1029/2008WR006948
46. Gutman G, Ignatov A. The derivation of the green vegetation fraction from NOAA/AVHRR data for use in numerical weather prediction models. International Journal of Remote Sensing, 1998, 19(8): 1533–1543
47. Sun Fubao, Yang Dawen, Liu Zhiyu, Cong Zhentao, Lei Zhidong. Validation of Coupled water-energy balance in the Haihe River basin and inland river basins. Journal of China Hydrology, 2007, 27 (2): 7–10 (in Chinese)
48. Yang Hanbo, Yang Dawen, Lei Zhidong, Lei Huimin. Derivation and verification of the coupled water-energy balance equation at arbitrary time scale. Journal of Hydraulic Engineering, 2008, 39 (5): 610–617 (in Chinese)
49. Bouchet R. Evapotranspiration reelle et potentielle, signification climatique. In: IAHS Publication No.62, 1963, 134–142